Published by :
https://www.ijert.org/
An International Peer-Reviewed Journal

International Journal of Engineering Research & Technology (IJERT)
ISSN: 2278-0181
Vol. 15 Issue 09 , September - 2026

Millet-Extract-Mediated Green Synthesis of Fe_2O_3 Nanoparticles for Visible-Light-Driven Photocatalytic Degradation of Rhodamine B

Bandi Ashok[1] , Bandari Raju[1], [2]M. Satyanarayana, [1]A. Rajasri
[1]Department of Physics, SRR Government Arts & Science College, Karimnagar-505 001
[2]Department of Physics, Government Degree College, Rajendranagar, Rangareddy, Hydereabad-505 218

Abstract - Iron oxide nanoparticles (Fe_2O_3NPs) were successfully synthesized through a sustainable green synthesis route employing aqueous extracts of finger millet, pearl millet, and foxtail millet. The naturally occurring phytochemicals in the millet extracts acted as reducing, capping, and stabilizing agents, facilitating the formation and stabilization of the nanoparticles. The synthesized Fe_2O_3NPs were systematically characterized using X-ray diffraction (XRD), scanning electron microscopy (SEM), energy-dispersive X-ray spectroscopy (EDX), and Fourier-transform infrared spectroscopy (FTIR). Their photocatalytic activity was investigated by monitoring the degradation of Rhodamine B (RhB) dye under visible-light irradiation. Among the synthesized materials, Fe_2O_3NPs prepared using finger millet extract exhibited the highest photocatalytic efficiency, achieving approximately %92degradation of RhB within 120min. The enhanced photocatalytic performance demonstrates the potential of the synthesized Fe_2O_3NPs as effective photocatalysts for the treatment of dye-contaminated wastewater. Furthermore, the utilization of readily available millet extracts provides a simple, economical, environmentally benign, and sustainable alternative to conventional chemical synthesis methods

***Key Words*: Green synthesis, Nanoparticles, Millet extract, Photocatalysis, RhB degradation**

I. INTRODUCTION

Nanomaterials have emerged as promising materials of scientific and technological importance owing to their distinctive physicochemical characteristics and diverse reaction pathways, offering considerable potential for addressing contemporary environmental and biomedical challenges [1–3]. Among the various classes of nanomaterials, iron oxide-based nanoparticles have received significant research interest because of their natural abundance, high surface-area-to-volume ratio, excellent chemical and thermal stability, and remarkable magnetic properties. These characteristics enable their application in several fields, including biomedicine, heterogeneous catalysis, environmental remediation, chemical sensing, cosmetics, and wastewater treatment. Several conventional techniques have been developed for the synthesis of iron-based nanomaterials, including chemical reduction, thermal decomposition, pyrolysis, photochemical and electrochemical methods, ultraviolet irradiation, laser ablation, and lithographic approaches [4,5].

Although these methods can produce nanoparticles with controlled properties, they commonly involve toxic or hazardous chemicals, including hydrazine, sodium borohydride, sodium citrate, and hydroxylamine, as reducing or stabilizing agents. The extensive use of such chemical reagents can result in undesirable environmental impacts and may pose potential risks to biological systems. Consequently, green synthesis strategies have gained considerable attention as safer and more sustainable alternatives for producing iron-based nanoparticles. These approaches generally offer advantages such as reduced environmental impact, lower energy consumption, simplicity, and cost-effectiveness. In particular, plant-mediated nanoparticle synthesis has become increasingly attractive because plants are readily available, renewable, and rich in naturally occurring phytochemicals. Plant extracts contain a diverse range of biologically active constituents, including polyphenols, flavonoids, proteins, terpenoids, tannins, alkaloids, and other antioxidant compounds. These phytochemicals can participate in nanoparticle formation by facilitating the reduction of metal ions while also contributing to particle stabilization and surface functionalization. Thus, plant-based synthesis provides an environmentally compatible route for the preparation of iron oxide nanoparticles with potential applications in environmental remediation and other advanced technologies.

II. MATERIALS AND METHODS

A. Materials

International Journal of Engineering Research & Technology (IJERT)
ISSN: 2278-0181
Vol. 15 Issue 09 , September - 2026

Millet grains (finger millet, pearl millet, foxtail millet) were procured from a local market. Ferric chloride ($FeCl_3$) and ferrous sulfate ($FeSO_4$) of analytical grade were used without further purification. Distilled water was used throughout the experiment

B. Preparation of Millet Extract

The millet grains were initially washed several times with distilled water to eliminate adhering impurities and subsequently dried at room temperature. The dried grains were then pulverized into a fine powder using a mechanical grinder. Approximately 10 g of the resulting millet powder was dispersed in 100 mL of distilled water and maintained at 70 °C for 20 min under heating. After cooling to room temperature, the suspension was filtered through Whatman No. 1 filter paper to remove insoluble residues and obtain a clear aqueous millet extract for further synthesis.

C. Synthesis of Iron Nanoparticles

For the green synthesis of Fe_2O_3 nanoparticles, 50 mL of a 0.05 M aqueous $FeCl_3$ solution was prepared as the iron precursor. Subsequently, 50 mL of the freshly prepared aqueous millet extract was added slowly, dropwise, to the $FeCl_3$ solution under continuous magnetic stirring at 60 °C. The reaction mixture was maintained under constant stirring for 45 min to facilitate the interaction of iron ions with the phytochemical constituents present in the millet extract. During the reaction, the color of the mixture gradually changed from pale brown to dark brown, indicating the formation of iron-based nanoparticles. The resulting suspension was then allowed to age at room temperature to promote further nucleation and stabilization of the nanoparticles. The product was subsequently separated, washed thoroughly with distilled water, dried, and calcined to obtain Fe_2O_3 nanoparticles for further characterization and photocatalytic studies.

III. RESULT AND DESCUSSION

A. XRD Analysis

The X-ray diffraction (XRD) patterns of the Fe_2O_3 nanoparticles synthesized using finger millet, pearl millet, and foxtail millet extracts are presented in Fig. 1. All three samples display well-defined diffraction reflections at approximately 24°, 33°, 35°, 49°, and 54° in the 2θ range.

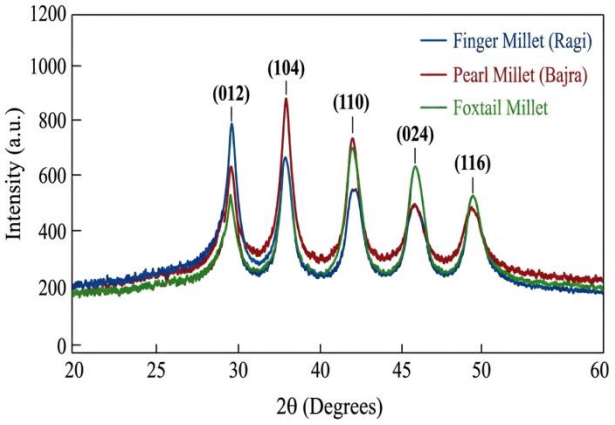

Fig-1. XRD of Iron oxide nanoparticles exctrcts of finger, pearl and foxtail millets

These reflections can be indexed to the (012), (104), (110), (024), and (116) crystallographic planes, respectively, and are characteristic of the rhombohedral hematite (α-Fe_2O_3) phase. The observed peak positions are consistent with the standard JCPDS reference pattern No. 33-0664, confirming the formation of crystalline α-Fe_2O_3 nanoparticles through the millet-mediated green synthesis route [4,6].

B. Scanning Electron Microscope (SEM)

The scanning electron microscopy (SEM) micrographs provide information on the surface morphology of the Fe_2O_3 nanoparticles synthesized using three different millet extracts, namely finger millet (Ragi), pearl millet (Bajra), and foxtail millet. As shown in Fig. 2(a), the Fe_2O_3 nanoparticles synthesized using finger millet extract exhibit a predominantly spherical morphology with relatively uniform particle distribution and smooth surfaces. The particles are well dispersed, with sizes mainly within the nanometer range of approximately 10–30 nm. Only a limited degree of particle agglomeration is observed, suggesting that the phytochemical constituents present in the finger millet extract may have contributed effectively to the capping and stabilization of the nanoparticles during synthesis [7–10].

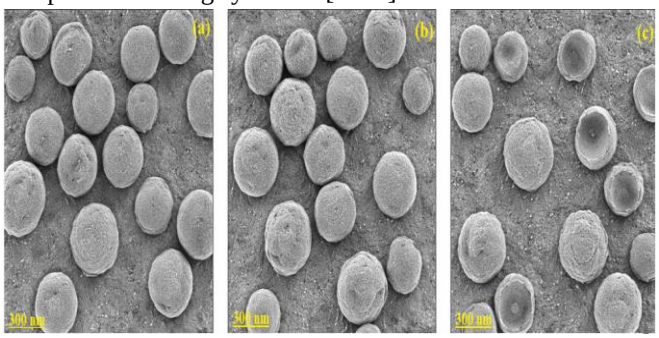

Fig-2. SEM of Iron oxide nanoparticles of (a) finger(b) pearl and(c) foxtail millets exctracts

International Journal of Engineering Research & Technology (IJERT)
ISSN: 2278-0181
Vol. 15 Issue 09 , September - 2026

The SEM image in Fig.2(b) reveals that the Fe_2O_3 nanoparticles synthesized using pearl millet (Bajra) extract possess predominantly spherical to semi-spherical morphology, with particle sizes ranging from approximately 20– 50nm. Compared with the nanoparticles obtained from finger millet extract, these particles are relatively larger and show a moderate degree of agglomeration, which may be attributed to the comparatively lower stabilization of the nanoparticles by phytochemical constituents present in the extract. In contrast, the Fe_2O_3nanoparticles synthesized using foxtail millet extract exhibit irregular and semi-spherical morphologies, along with partially hollow structures and pronounced aggregation. The particles display a broader size distribution and comparatively lower uniformity, suggesting that the phytochemicals in the foxtail millet extract provide less effective capping and stabilization during nanoparticle formation [11,.[12

C. Energy Dispersive X-ray (EDX) spectra

The Energy-Dispersive X-ray (EDX) spectra shown in Fig. 3 provide evidence of the elemental composition of the iron oxide nanoparticles synthesized using the extracts of three different millets, namely finger millet (Ragi), pearl millet (Bajra), and foxtail millet

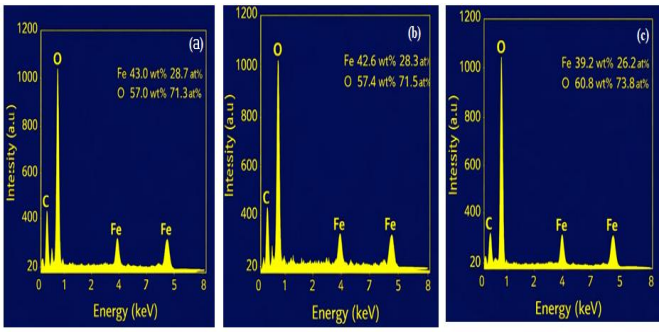

Fig-3. EDX of Iron oxide nanoparticles of (a) finger(b) pearl and(c) foxtail millets exctracts

D. Fourier transform infrared Spectra (FTIR)

The FTIR spectra of the iron oxide (Fe_2O_3) nanoparticles synthesized using finger millet (Ragi), pearl millet (Bajra), and foxtail millet extracts provide valuable information regarding the functional groups involved in nanoparticle synthesis and stabilization. As illustrated in Fig. 4, all three samples display a broad absorption band near 3400 cm^{-1}, which can be attributed to O–H stretching vibrations associated with phenolic and alcoholic groups. The absorption bands observed around 2920 cm^{-1} are assigned to C–H stretching vibrations, while the band near 1650 cm^{-1} can be related to C=O stretching vibrations of protein-associated groups. The band appearing at approximately 1380 cm^{-1} corresponds to C–N stretching, whereas the absorption around 1150 cm^{-1} is associated with C–O stretching vibrations of polysaccharide-related compounds. These characteristic bands indicate the participation of various phytochemicals and biomolecules present in the millet extracts during nanoparticle formation. In addition, the absorption band observed in the 550–600 cm^{-1} region is attributed to Fe–O vibrational modes, providing evidence for the formation of iron oxide nanoparticles [12].

Among the three samples, the nanoparticles synthesized with finger millet extract exhibit relatively intense and well-defined FTIR bands, suggesting a greater contribution of phytochemical constituents to the reduction and stabilization processes. The pearl millet-derived nanoparticles display intermediate peak intensities, whereas the foxtail millet sample shows comparatively broader and less intense absorption bands, which may indicate differences in phytochemical composition and capping ability. Overall, the FTIR findings demonstrate that biomolecules present in millet extracts contribute significantly to the green synthesis of Fe_2O_3 nanoparticles by acting as both reducing and stabilizing/capping agents [13–15].

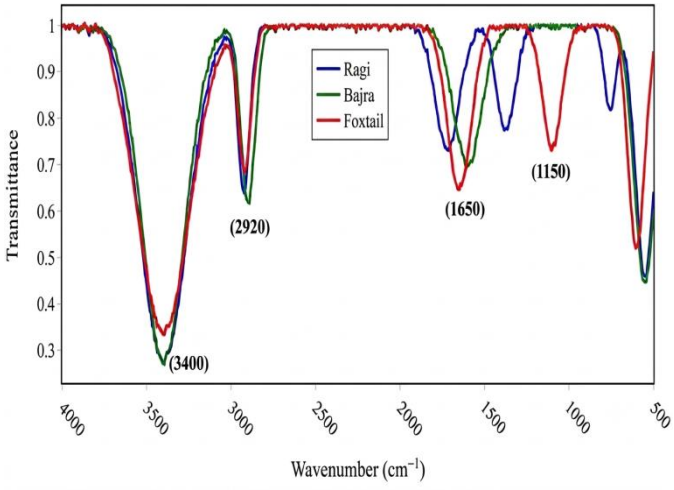

Fig-4. FTIR spectra of Iron oxide nanoparticles of all millets exctracts

International Journal of Engineering Research & Technology (IJERT)
ISSN: 2278-0181
Vol. 15 Issue 09 , September - 2026

IV. PHOTOCATALYSIS

The photocatalytic performance of the Fe_2O_3 nanoparticles synthesized using finger millet (Ragi), pearl millet (Bajra), and foxtail millet extracts was investigated by monitoring the degradation of Rhodamine B (RhB), a widely studied organic dye pollutant, under visible-light irradiation using a 300 W lamp. As shown in Fig. 5(a), the RhB solution without a photocatalyst exhibited only about 10 % degradation, indicating that direct photolysis under the employed irradiation conditions was negligible. In contrast, the Fe_2O_3 nanoparticles prepared with the different millet extracts demonstrated considerably enhanced photocatalytic activity, although their efficiencies varied depending on the extract employed during synthesis. The Fe_2O_3 nanoparticles synthesized using finger millet extract exhibited the highest degradation efficiency, reaching approximately 92% after 240 min of visible-light irradiation, as presented in Fig. 5(b). This was followed by the nanoparticles synthesized using pearl millet and foxtail millet extracts, which achieved degradation efficiencies of about 85% and 78%, respectively.

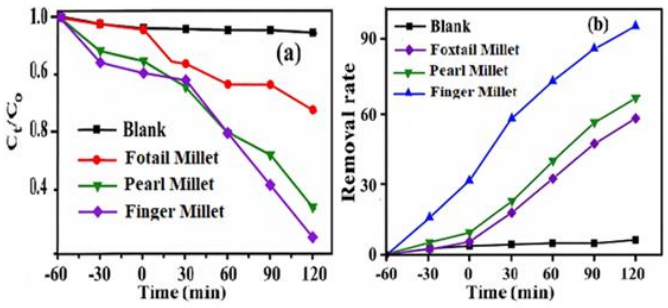

Fig-5. Concentration changes of Rh B over Iron oxidenanoparticles of millets exctracts along with the blank experiment. **(b).** Degradation % of Rh B in the presence of Iron oxidenanoparticles of millets exctracts along with pure Rh B.

Figure 6(a–b) presents the time-dependent UV-Vis absorption profiles used to monitor the photocatalytic performance of Iron oxidenanoparticles of finger millets exctracts which are show highest PCA against Rh B under visible-light illumination. The steady, pronounced attenuation of the characteristic Rh B.absorption peak with increasing exposure time directly demonstrates the progressive breakdown of the dye's chromophoric structure. This continuous decline in absorbance intensity confirms the active visible-light-driven degradation of Rh B.while the comparative curves in Figure 6(a) and 6(b) clearly illustrate the relative kinetic efficiencies and superior catalytic performance Iron oxidenanoparticlesof finger millets exctracts

The enhanced photocatalytic performance of the finger millet-mediated Fe_2O_3 nanoparticles may be associated with their relatively smaller particle size, greater accessible surface area, and increased availability of surface-active sites. These characteristics can promote more effective interaction between the photocatalyst and RhB molecules and facilitate the generation of reactive oxygen species (ROS), particularly hydroxyl radicals (•OH) and superoxide radicals (O_2^{-}•), under visible-light irradiation. The generated reactive species contribute to the oxidative decomposition of RhB into smaller and potentially less harmful intermediates.

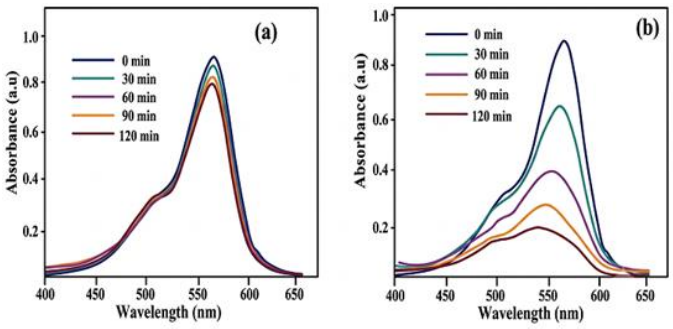

Fig-6. UV-VIS absorption spectra of)a (Pure RhB)b (RhB with Iron oxide nanoparticlesof finger millets exctracts

The comparatively lower photocatalytic efficiencies of the pearl millet- and foxtail millet-derived nanoparticles may be related to greater particle aggregation and reduced accessibility of active surface sites. Overall, the results indicate that the type of millet extract used during green synthesis has a significant influence on the physicochemical characteristics and photocatalytic behavior of Fe_2O_3 nanoparticles. Among the investigated extracts, finger millet exhibited the most favorable performance as a biogenic reducing and stabilizing medium for producing Fe_2O_3 nanoparticles with promising potential for photocatalytic environmental remediation [14–17].

V. SCAVENGER TEST

The scavenger experiments conducted with the millet-mediated Fe_2O_3 nanoparticles provide valuable insight into the reactive species involved in the

International Journal of Engineering Research & Technology (IJERT)
ISSN: 2278-0181
Vol. 15 Issue 09 , September - 2026

photocatalytic degradation of Rhodamine B. As shown in Fig. 7, the addition of benzoquinone (BQ) resulted in the most pronounced decrease in degradation efficiency for the finger millet (Ragi)-mediated Fe_2O_3 nanoparticles, which exhibited the highest photocatalytic performance.

This significant inhibition indicates that superoxide radicals (O_2^{-}•) are the predominant reactive species contributing to RhB degradation. The introduction of isopropanol (IPA) also caused a substantial reduction in photocatalytic efficiency, demonstrating the important contribution of hydroxyl radicals (•OH) to the degradation process.

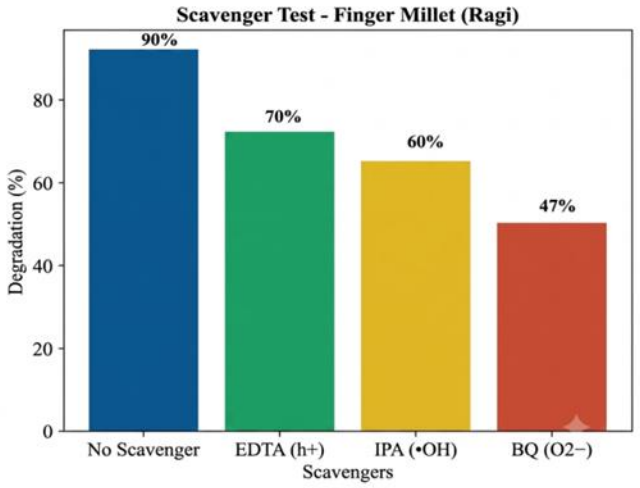

Fig-7. Scavenger test of RhB with Iron oxide nanoparticlesof finger millets exctracts

In comparison, the presence of EDTA produced a relatively smaller decline in degradation efficiency, suggesting that photogenerated holes (h^+) have a comparatively secondary role in the photocatalytic reaction. Among the synthesized samples, the Ragi-mediated Fe_2O_3 nanoparticles demonstrated the highest photocatalytic activity, followed by the Bajra- and foxtail millet-derived nanoparticles, consistent with the degradation trends observed in the photocatalytic experiments [18–19].

VI. CONCLUSION

The present investigation establishes an effective green synthesis route for iron oxide nanoparticles using extracts of finger millet (Ragi), pearl millet (Bajra), and foxtail millet. This biological approach offers a simple, economical, and environmentally benign alternative to conventional nanoparticle synthesis, with naturally occurring phytochemicals serving as reducing and capping agents. The resulting nanoparticles exhibited notable photocatalytic efficiency toward Rhodamine B degradation under visible-light irradiation, achieving removal efficiencies of 92%, 85%, and 78% for the Ragi-, Bajra-, and foxtail millet-derived nanoparticles, respectively. Scavenger experiments indicated that benzoquinone produced the greatest suppression of photocatalytic activity, suggesting that superoxide radicals (O_2^{-}•) are the major reactive species involved in RhB degradation, while hydroxyl radicals (•OH) and photogenerated holes (h^+) also contribute to the reaction. Among the investigated samples, the Ragi-mediated Fe_2O_3 nanoparticles exhibited the highest photocatalytic performance, followed by the Bajra- and foxtail millet-derived materials. These findings demonstrate that the choice of millet extract plays an important role in determining the properties and photocatalytic performance of the synthesized nanoparticles, highlighting their potential application in sustainable wastewater treatment and environmental remediation.

REFERENCES

[1] Iravani, S. (2011). Green synthesis of metal nanoparticles using plants. Chemical Society Reviews, 40, 208–218.
[2] Ahmed, S., Ahmad, M., Swami, B. L., & Ikram, S. (2016). A review on plants extract mediated synthesis of silver nanoparticles. Journal of Advanced Research, 7, 17–28.
[3] Nasrollahzadeh, M., Sajadi, S. M., & Atarod, M. (2019). Green synthesis of metal nanoparticles using plant extracts and their applications. Journal of Cleaner Production, 231, 596–611.
[4] Gupta, A. K., & Gupta, M. (2005). Synthesis and surface engineering of iron oxide nanoparticles for biomedical applications. Biomaterials, 26, 3995–4021.
[5] R. M., & Schwertmann, U. (2003). The iron oxides: structure, properties, reactions, occurrences and uses. Wiley-VCH.
[6] Sharma, V. K., Yngard, R. A., & Lin, Y. (2009). Silver nanoparticles: Green synthesis and their antimicrobial activities. Advances in Colloid and Interface Science, 145, 83–96.
[7] Singh, J., Dutta, T., Kim, K. H., Rawat, M., Samddar, P., & Kumar, P. (2018). 'Green' synthesis of metals and their oxide nanoparticles: applications for environmental remediation. Journal of Nanobiotechnology, 16, 84.
[8] Zhang, N., Zhang, Y., & Xu, Y. J. (2012). Recent progress on graphene-based photocatalysts: current status and future perspectives. Nanoscale, 4, 5792–5813.
[9] Karthikeyan, C., et al. (2020). Green synthesis of iron oxide nanoparticles using plant extracts and their photocatalytic activity. Environmental Science and Pollution Research, 27, 12357–12367.
[10] Ali, A., Zafar, H., Zia, M., ul Haq, I., Phull, A. R., Ali, J. S., & Hussain, A. (2016). Synthesis, characterization, applications, and challenges of iron oxide nanoparticles. Nanotechnology, Science and Applications, 9, 49–67

International Journal of Engineering Research & Technology (IJERT)
ISSN: 2278-0181
Vol. 15 Issue 09 , September - 2026

[11] Pham, X. N., Nguyen, T. P., & Nguyen, T. D. (2016). Green synthesis of iron nanoparticles using plant extract. Materials Letters, 181, 173–177.
[12] Mittal, A. K., Chisti, Y., & Banerjee, U. C. (2013). Synthesis of metallic nanoparticles using plant extracts. Biotechnology Advances, 31, 346–356.
[13] Ramesh, M., et al. (2015). Green synthesis of Fe_2O_3 nanoparticles and their catalytic activity. Applied Surface Science, 356, 1281–1286
[14] Zhang, N., Zhang, Y., & Xu, Y. J. (2012). Graphene-based photocatalysts. Nanoscale, 4, 5792–5813
[15] Wang, J., & Wang, S. (2020). Removal of organic pollutants using photocatalysis. Chemical Engineering Journal, 382, 122–135.
[16] Chong, M. N., Jin, B., Chow, C. W. K., & Saint, C. (2010). Recent developments in photocatalytic water treatment. Water Research, 44, 2997–3027.
[17] Daneshvar, N., Salari, D., & Khataee, A. R. (2004). Photocatalytic degradation of azo dyes. Journal of Photochemistry and Photobiology A, 162, 317–322.
[18] Kumar, B., Smita, K., & Cumbal, L. (2014). Plant-mediated synthesis of nanoparticles. Journal of Saudi Chemical Society, 18, 364–373.
[19] Yadav, R., et al. (2017). Green synthesis of iron nanoparticles using plant extracts. Journal of Environmental Chemical Engineering, 5, 500–507.
[20] Tran, N., & Webster, T. J. (2010). Nanotechnology for biomedical applications. International Journal of Nanomedicine, 5, 277–283.